

ArbiLoMod: Local Solution Spaces by Random Training in Electrodynamics

Andreas Buhr, Christian Engwer, Mario Ohlberger, and Stephan Rave

Abstract The simulation method ArbiLoMod [1] has the goal of providing users of Finite Element based simulation software with quick re-simulation after localized changes to the model under consideration. It generates a Reduced Order Model (ROM) for the full model without ever solving the full model. To this end, a localized variant of the Reduced Basis method is employed, solving only small localized problems in the generation of the reduced basis. The key to quick re-simulation lies in recycling most of the localized basis vectors after a localized model change. In this publication, ArbiLoMod's local training algorithm is analyzed numerically for the non-coercive problem of time harmonic Maxwell's equations in 2D, formulated in $H(\text{curl})$.

1 Introduction

Simulation software based on the Finite Element Method is an essential ingredient of many engineering workflows. In their pursue of design goals, engineers often simulate structures several times, applying small changes after each simulation. This results in large similarities between subsequent simulation runs. These similarities are usually not considered by simulation software. The simulation method ArbiLoMod was designed to change that and accelerate the subsequent simulation of geometries which only differ in small details. A motivating example is the design of mainboards for PCs. Improvements in the signal integrity properties of e.g. DDR memory channels is often obtained by localized changes, as depicted in Fig. 1.

Andreas Buhr e-mail: andreas@andreasbuhr.de · Christian Engwer e-mail: christian.engwer@uni-muenster.de · Mario Ohlberger e-mail: mario.ohlberger@uni-muenster.de · Stephan Rave e-mail: stephan.rave@uni-muenster.de
Institute for Computational and Applied Mathematics, University of Münster, Einsteinstraße 62, D-48149 Münster, Germany

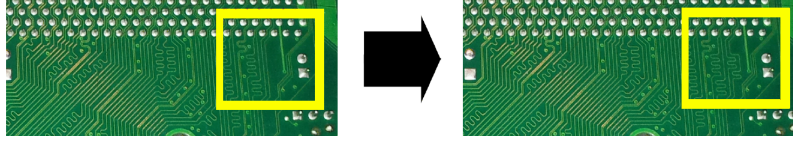


Fig. 1 Printed circuit board subject to local modification of conductive tracks.

ArbiLoMod was also designed with the available computing power in mind: Today, cloud environments are just a few clicks away and everyone can access hundreds of cores easily. However, the network connection to these cloud environments is relatively slow in comparison to the available computing power, so a method which should perform well under these circumstances must be designed to be communication avoiding.

At the core of ArbiLoMod lies a localized variant of the Reduced Basis Method. The Reduced Basis Method is a well established approach to create reduced order models (ROMs) and its application to the Maxwell's equations has been extensively investigated by many groups (see e.g. [5, 10, 2, 20, 9]). On the other hand, there are lots of methods with localized basis generation (e.g. [12, 11, 19, 13, 7, 21, 18]). However to the authors' knowledge, only little was published on the combination of both. In [4], the Reduced Basis Element Method is applied to time harmonic Maxwell's equations.

This publication evaluates ArbiLoMod's training numerically for the time harmonic Maxwell's equation. The remainder of this article is structured as follows: In the following Section 2, the problem setting is given. Section 3 outlines ArbiLoMod and highlights the specialties when considering inf-sup stable problems in $H(\text{curl})$. Afterwards, we demonstrate ArbiLoMod's performance on a numerical example in Section 4. Finally, we conclude in Section 5.

2 Problem Setting

We consider Maxwell's equations [14] on the polygonal domain Ω . The material is assumed to be linear and isotropic, i.e. the electric permittivity ε and the magnetic permeability μ are scalars. On the boundary $\partial\Omega = \Gamma_R \cup \Gamma_D$ we impose Dirichlet ($E \times n = 0$ on Γ_D) and Robin ($H \times n = \kappa(E \times n) \times n$ on Γ_R , [16, eq. (1.18)]) boundary conditions with the surface impedance parameter κ . n denotes the unit outer normal of Ω . The excitation is given by a current density \hat{j} .

For the time harmonic case, this results in the following weak formulation: find $u \in V := H(\text{curl})$ so that

$$\begin{aligned} a(u, v; \omega) &= f(v; \omega) \quad \forall v \in V, \\ a(u, v; \omega) &:= \int_{\Omega} \frac{1}{\mu} (\nabla \times u) \cdot (\nabla \times \bar{v}) - \varepsilon \omega^2 (u \cdot \bar{v}) dv + i\omega\kappa \int_{\Gamma_R} (u \times n) \cdot (\bar{v} \times n) dS, \end{aligned} \quad (1)$$

$$f(v; \omega) := -i\omega \int_{\Omega} (\hat{j} \cdot \bar{v})$$

where ω is the angular frequency. We see ω as a parametrization to this problem. We solve in a parameter domain sampled by a finite training set Ξ .

We use the inner product and energy norm given by:

$$\begin{aligned} (v, u)_V &:= \int_{\Omega} \frac{1}{\mu} (\nabla \times u) \cdot (\nabla \times \bar{v}) + \varepsilon \omega_{\max}^2 (u \cdot \bar{v}) dv + \omega_{\max} \kappa \int_{\Gamma_R} (u \times n) \cdot (\bar{v} \times n) dS, \\ \|u\|_V &:= \sqrt{(u, u)_V}. \end{aligned} \quad (2)$$

2.1 Discretization

We assume there is a non overlapping domain decomposition with subdomains Ω_i , $\Omega_i \cap \Omega_j = \emptyset$ for $i \neq j$. For simplicity, we assume it to be rectangular. The domain decomposition should cover the problem domain $\Omega \subseteq \bigcup_i \Omega_i$ but the subdomains need not resolve the domain. This is important as we want to increase or decrease the size of Ω between simulation runs without changing the domain decomposition. For example, in a printed circuit board (PCB), the metal traces are often simulated as being outside of the domain. Thus, a change of the traces leads to a change of the calculation domain.

Further we assume there is a triangulation of Ω which resolves the domain decomposition. We denote by V_h the discrete space spanned by lowest order Nedelec ansatz functions [17] on this triangulation.

3 ArbiLoMod for Maxwell's Equations

The main ingredients of ArbiLoMod are (1) a localizing space decomposition, (2) localized trainings for reduced local subspace generation, (3) a localized a-posteriori error estimator and (4) a localized enrichment for basis improvement. In this publication, we focus on the first two steps, which are described in the following.

3.1 Space Decomposition

Localization is performed in ArbiLoMod using a direct decomposition of the ansatz space into localized subspaces. In the 2D case with Nedelec ansatz functions, there are only volume spaces $V_{\{i\}}$ associated with the subdomains Ω_i , and interface spaces $V_{\{i,j\}}$ associated with the interfaces between Ω_i and Ω_j . The interface spaces are only associated with an interface, they are subspaces of the global function space

and have support on two domains. They are not trace spaces. In higher space dimensions and/or with different ansatz functions, there may be also spaces associated with edges and nodes of the domain decomposition [1].

$$V_h = \left(\bigoplus_i V_{\{i\}} \right) \oplus \left(\bigoplus_{i,j} V_{\{i,j\}} \right) \quad (3)$$

The spaces $V_{\{i\}}$ are simply defined as the span of all ansatz functions having support only on Ω_i . With \mathcal{B} denoting the set of all FE basis functions, we define:

$$V_{\{i\}} := \text{span} \{ \psi \in \mathcal{B} \mid \text{supp}(\psi) \subseteq \bar{\Omega}_i \}. \quad (4)$$

The interface spaces $V_{\{i,j\}}$ are not simply the span of FE ansatz functions. Instead, they are defined as the span of all ansatz functions on the interface plus their extension to the adjacent subdomains. The extension is done by solving for a fixed frequency ω' with Dirichlet zero boundary conditions. The formal definition of the interface spaces is in two steps: First, we define $U_{\{i,j\}}$ as the space spanned by all ansatz function having support on both Ω_i and Ω_j :

$$U_{\{i,j\}} := \text{span} \{ \psi \in \mathcal{B} \mid \text{supp}(\psi) \cap \Omega_i \neq \emptyset, \text{supp}(\psi) \cap \Omega_j \neq \emptyset \}. \quad (5)$$

Then we define the extension operator:

$$\begin{aligned} \text{Extend} : U_{\{i,j\}} &\rightarrow V_{\{i\}} \oplus U_{\{i,j\}} \oplus V_{\{j\}}, \\ \varphi &\mapsto \varphi + \psi \\ &\text{where } \psi \in V_{\{i\}} \oplus V_{\{j\}} \text{ solves} \\ &a(\varphi + \psi, \phi; \omega') = 0 \quad \forall \phi \in V_{\{i\}} \oplus V_{\{j\}}. \end{aligned} \quad (6)$$

We then can define the interface spaces as

$$V_{\{i,j\}} := \{ \text{Extend}(\varphi) \mid \varphi \in U_{\{i,j\}} \}. \quad (7)$$

Equation (3) holds for this decomposition, i.e. there is a unique decomposition of every element of V_h into the localized subspaces. We define projection operators $P_{\{i\}} : V_h \rightarrow V_{\{i\}}$ and $P_{\{i,j\}} : V_h \rightarrow V_{\{i,j\}}$ by the relation

$$\varphi = \sum_i P_{\{i\}}(\varphi) + \sum_{i,j} P_{\{i,j\}}(\varphi) \quad \forall \varphi \in V_h. \quad (8)$$

3.2 Training

Having defined the localized spaces, we create reduced localized subspaces $\tilde{V}_{\{i\}} \subseteq V_{\{i\}}$ and $\tilde{V}_{\{i,j\}} \subseteq V_{\{i,j\}}$ by a localized training procedure. The training is inspired by

the ‘‘Empirical Port Reduction’’ introduced by Eftang et.al.[8]. Its main four steps are:

1. solve the problem (1) on a small training domain around the space in question with zero boundary values for all parameters in the training set Ξ ,
2. solve the homogeneous equation repeatedly on a small training domain around the space in question with random boundary values for all parameters in Ξ ,
3. apply the space decomposition to all computed local solutions to obtain the part belonging to the space in question and
4. use a greedy procedure to create a space approximating this set.

For further details, we refer to [1]. The small training domain for an interface space consists of the six subdomains around that interface. The small training domain for a volume space consists of nine subdomains: the subdomain in question and the eight subdomains surrounding it.

While the ‘‘Empirical Port Reduction’’ in [8] generates an interface space and requires ports which do not intersect, this training can be used for both interface and volume spaces. It can handle touching ports and can thus be applied to a standard domain decomposition.

3.3 Reduced Model

In these first experiments the reduced global problem is obtained by a simple Galerkin projection onto the direct sum of all reduced local subspaces. The global solution space is

$$\tilde{V}_h := \left(\bigoplus_i \tilde{V}_{\{i\}} \right) \oplus \left(\bigoplus_{i,j} \tilde{V}_{\{i,j\}} \right). \quad (9)$$

And the reduced problem reads: find $\tilde{u} \in \tilde{V}_h$ such that

$$a(\tilde{u}, v; \mu) = f(v) \quad \forall v \in \tilde{V}_h. \quad (10)$$

4 Numerical Example

The numerical experiments are performed with pyMOR [15]. The source code used to reproduce the results in this publication is provided alongside with this publication and can be downloaded at <http://www.arbilomod.org/morepas2015.tgz>. See the README file therein for installation instructions.

4.1 Geometry Simulated

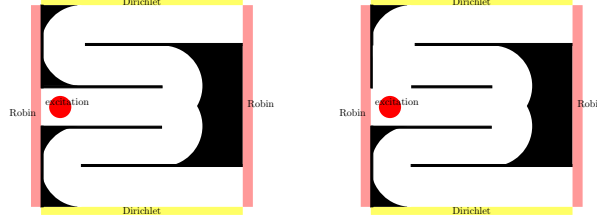


Fig. 2 Geometries simulated. Black area is not part of the domain and treated as Dirichlet zero boundary. Note the change is topology changing.

We simulate the unit square $(0, 1) \times (0, 1)$ with robin boundary conditions at $\Gamma_R := 0 \times (0, 1) \cup 1 \times (0, 1)$ and Dirichlet zero boundary conditions at $\Gamma_D := (0, 1) \times 0 \cup (0, 1) \times 1$. The surface impedance parameter κ is chosen as the impedance of free space, $\kappa = 1/376.73$ Ohm. We introduce some structure by inserting perfect electric conductors (PEC) into the domain, see Fig. 2. The PEC is modeled as Dirichlet zero boundary condition. Note that it is slightly asymmetric intentionally, to produce more interesting behavior. The mesh does not resolve the geometry. Rather, we use a structured mesh and remove all degrees of freedom which are associated with an edge whose center is inside of the PEC structure. The structured mesh consists of 100 times 100 squares, each of which is divided into four triangles. With each edge, one degree of freedom is associated, which results in 60200 degrees of freedom, some of which are “disabled” because they are in PEC or on a Dirichlet boundary. The parameter domain is the range from 10 MHz to 1 GHz. For the training set Ξ , we use 100 equidistant points in this range, including the endpoints. To simulate an “arbitrary local modification”, the part of the PEC within $(0.01, 0.2) \times (0.58, 0.80)$ is removed and the simulation domain is enlarged.

The excitation is a current

$$j(x, y) := \exp\left(-\frac{(x-0.1)^2 + (y-0.5)^2}{1.25 \cdot 10^{-3}}\right) \cdot \mathbf{e}_y \quad (11)$$

To get an impression of the solutions, some example solutions are plotted in Fig. 3.

4.2 Global Properties of Example

Before analyzing the behavior of the localized model reduction, we discuss some properties of the full model. For its stability, its continuity constant γ and reduced inf-sup constants $\tilde{\beta}$ are the primary concern. They guarantee existence and unique-

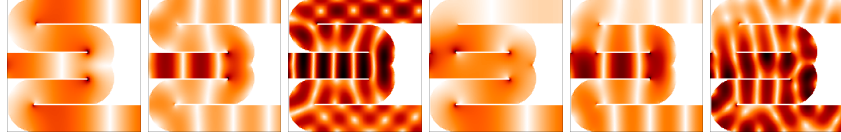


Fig. 3 Example solutions for $f=186$ MHz, $f=561$ MHz and $f=1$ GHz for the first and second geometry. Plotted is $|\text{Re}(E)|$. Script: `maxwell_create_solutions.py`

ness of the solution and their quotient enters the best-approximation inequality

$$\|u - \tilde{u}\| \leq \left(1 + \frac{\gamma}{\beta}\right) \inf_{v \in V_h} \|u - v\| \quad (12)$$

where u is the solution in V_h . Due to the construction of the norm, the continuity constant cannot be larger than one, and numerics indicate that it is usually one (Fig. 4). The inf-sup constant approaches zero when the frequency goes to zero. This is the well known low frequency instability of this formulation. There are remedies to this problem, but they are not considered here. The order of magnitude of the inf-sup constant is around 10^{-2} : Due to the Robin boundaries, the problem is stable. With Dirichlet boundaries only, the inf-sup constant would drop to zero at several frequencies. There are two drops in the inf-sup constant at ca. 770 MHz and 810 MHz. These correspond to resonances in the structure which arise when half a wavelength is the width of a channel ($\lambda/2 \approx 1/5$).

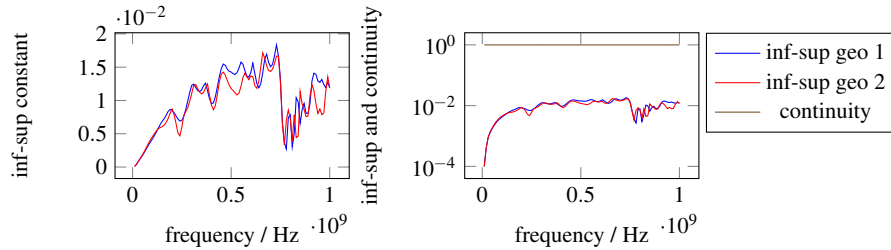


Fig. 4 inf-sup and continuity constant of bilinear form. Linear and logarithmic. Script: `maxwell_calculate_infsup.py`

The most important question for the applicability of any reduced basis method is: is the system reducible at all, i.e. can the solution manifold be approximated with a low dimensional solution space? The best possible answer to this question is the Kolmogorov n -width. We measured the approximation error when approximating the solution manifold with a basis generated by a greedy algorithm. The approximation is done by orthogonal projection onto the basis. This error is an upper bound to

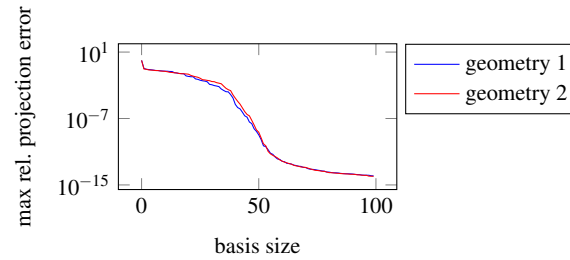


Fig. 5 Error when approximating the solution set for all $f \in \Xi$ with an n -dimensional basis obtained by greedy approximation of this set. This is an upper bound for the Kolmogorov n -width. Script: maxwell_global_n_width.py

the Kolmogorov n -width. Already with a basis size of 38, a relative error of 10^{-4} can be achieved, see Fig. 5. So this problem is well suited for reduced basis methods.

4.3 Properties of Localized Spaces

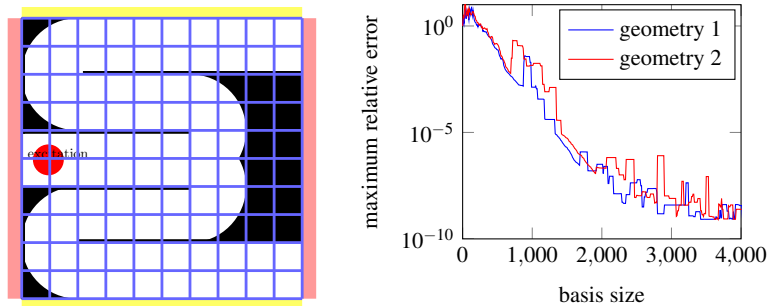


Fig. 6 Left: Domain decomposition used. Right: Maximum error when solving with a localized basis, generated by global solves. Script maxwell_local_n_width.py.

The next question is: how much do we lose by localization? Using basis vectors with limited support, one needs a larger total number of basis functions. To quantify this, we compare the errors with global approximation from the previous section with the error obtained when solving with a localized basis, using the best localized basis we can generate. We use a 10×10 domain decomposition (see Fig. 6 left) and the space decomposition introduced in Section 3.1. To construct the best possible basis, we solve the full problem for all parameters in the training set. For each local subspace, we apply the corresponding projection operator $P_{\{i\}} / P_{\{i,j\}}$ to all global solutions and subsequently generate a basis for these local parts of global

solutions using a greedy procedure. The error when solving in the resulting reduced space is depicted in Fig. 6, right. Much more basis vectors are needed, compared to the global reduced basis approach. However the reduction in comparison to the full model (60200 dofs) is still significant and in contrast to standard reduced basis methods, the reduced system matrix is not dense but block-sparse. For a relative error of 10^{-4} , 1080 basis vectors are necessary.

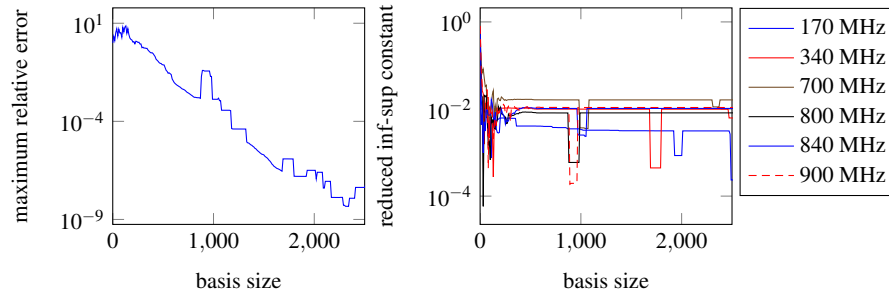


Fig. 7 Comparison of maximum error over all frequencies with inf-sup constant of reduced system at selected frequencies for geometry 1. Basis generated by global solves. Increased error and reduced inf-sup constant around basis size of 900. Script: maxwell_infsup_during_reduction.py

In Fig. 6 the error is observed to jump occasionally. This is due to the instability of a Galerkin projection of an inf-sup stable problem. While coercivity is retained during Galerkin projection, inf-sup stability is not. While the inf-sup constant of the reduced system is observed to be the same as the inf-sup constant of the full system most of the time, sometimes it drops. This is depicted in Fig. 7. For a stable reduction, a different test space is necessary. However, the application of the known approaches such as [3, 6] to the localized setting is not straightforward. The development of stable test spaces in the localized setting is beyond the scope of this publication.

4.4 Properties of Training

Local basis vectors should be generated using the localized training described in Section 3.2 and in [1]. To judge on the quality of these basis vectors, we compare the error obtained using these basis vectors with the error obtained with local basis vectors generated by global solves. The local basis vectors generated by global solves are the reference: These are the best localized basis we can generate. The results for both geometries are depicted in Fig. 8. While the error decreases more slowly, we still have reasonable basis sizes with training. For a relative error of 10^{-4} , 1280 basis vectors are necessary for geometry 1 and 1380 are necessary for geometry 2.

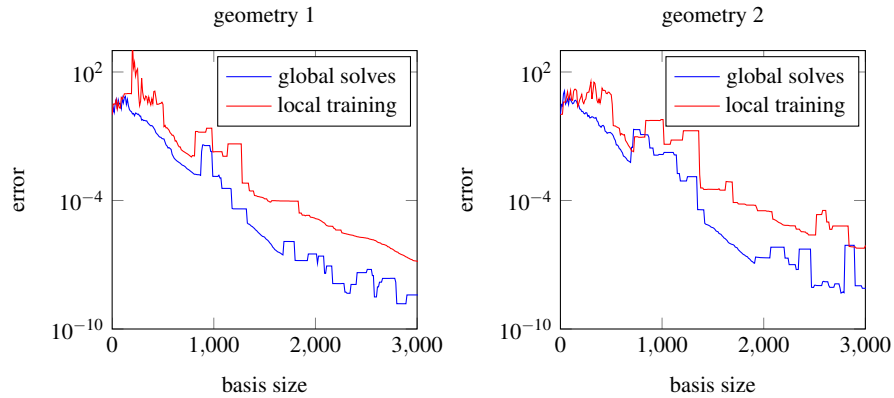


Fig. 8 Maximum error over all frequencies for both geometries. Basis generated by global solves vs. basis generated by local training. Script: maxwell_training_benchmark.py

4.5 Application to Local Geometry Change

If we work with a relative error of 5%, a basis of size 650 is sufficient for the first geometry and size 675 for the second. After the geometry change, the local reduced spaces which have no change in their training domain can be reused. Instead of solving the full system with 60200 degrees of freedom, the following effort is necessary per frequency point (see also Fig. 9). Because the runtime is dominated by matrix factorizations, we focus on these.

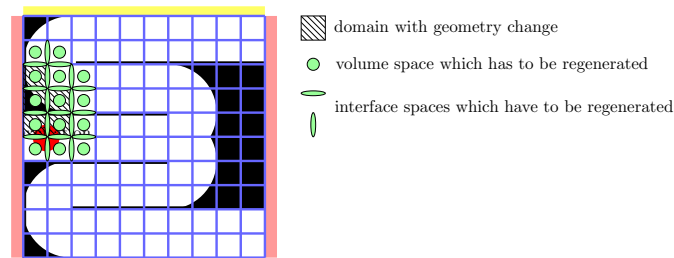


Fig. 9 Impact of geometry change: 5 domains contain changes, 14 domain spaces and 20 interface spaces have to be regenerated.

- 14 factorizations of local problems with 5340 dofs (volume training)
- 20 factorizations of local problems with 3550 dofs (interface training)
- 1 factorization of global reduced problem with 675 dofs (global solve)

The error between the reduced solution and the full solution in this case is 4.3%.
 Script to reproduce: `experiment_maxwell_geochange.py`. The spacial distribution of basis sizes is depicted in Fig. 10.

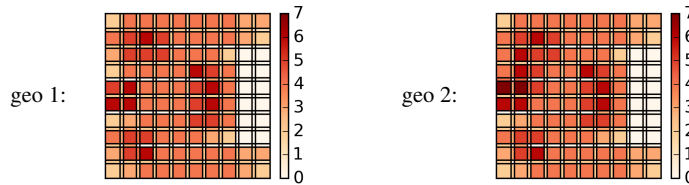


Fig. 10 Basis size distribution. Script: `postprocessing_draw_basis_sizes_maxwell_geochange.py`

5 Conclusion

ArbiLoMod was applied to the non-coercive problem of 2D Maxwell's equations in $H(\text{curl})$. Its localized training generates a basis of good quality. A reduced model with little error for the full problem can be generated using only local solves, which can easily be parallelized. After localized changes to the model, only in the changed region the localized bases have to be regenerated. All other bases can be reused, which results in large computational savings compared to a simulation from scratch. The amount of savings is very dependent of the model and the changes which are made. A thorough analysis of the computational savings is subject to future work, as is the adaptation of ArbiLoMod's localized a-posteriori error estimator and online enrichment to this problem as well as the instability of the Galerkin projection.

Acknowledgments

Andreas Buhr was supported by CST - Computer Simulation Technology AG. Stephan Rave was supported by the German Federal Ministry of Education and Research (BMBF) under contract number 05M13PMA.

References

1. Andreas Buhr, Christian Engwer, Mario Ohlberger, and Stephan Rave. ArbiLoMod, a simulation technique designed for arbitrary local modifications. *arXiv e-prints*, (1512.07840), December 2015. <http://arxiv.org/abs/1512.07840>.

2. Stefan Burgard, Alexander Sommer, Ortwin Farle, and Romanus Dyczij-Edlinger. Reduced-order models of finite-element systems featuring shape and material parameters. *Electromagnetics*, 34(3-4):143–160, 2014.
3. Kevin Carlberg, Charbel Bou-Mosleh, and Charbel Farhat. Efficient non-linear model reduction via a least-squares petrov–galerkin projection and compressive tensor approximations. *International Journal for Numerical Methods in Engineering*, 86(2):155–181, 2011.
4. Yanlai Chen, Jan S. Hesthaven, and Yvon Maday. *Spectral and High Order Methods for Partial Differential Equations: Selected papers from the ICOSAHOM '09 conference, June 22-26, Trondheim, Norway*, chapter A Seamless Reduced Basis Element Method for 2D Maxwell's Problem: An Introduction, pages 141–152. Springer, Berlin, Heidelberg, 2011.
5. Yanlai Chen, Jan S. Hesthaven, Yvon Maday, and Jernimo Rodriguez. Certified reduced basis methods and output bounds for the harmonic Maxwell's equations. *SIAM Journal on Scientific Computing*, 32(2):970–996, Jan 2010.
6. Wolfgang Dahmen, Christian Plesken, and Gerrit Welper. Double greedy algorithms: reduced basis methods for transport dominated problems. *ESAIM: Mathematical Modelling and Numerical Analysis*, 48(03):623–663, 2014.
7. Yalchin Efendiev, Juan Galvis, and Thomas Y. Hou. Generalized multiscale finite element methods (GMsFEM). *Journal of Computational Physics*, January 2013.
8. Jens L Eftang and Anthony T Patera. Port reduction in parametrized component static condensation: approximation and a posteriori error estimation. *International Journal for Numerical Methods in Engineering*, 96(5):269–302, Jul 2013.
9. M'Barek Fares, Jan S. Hesthaven, Yvon Maday, and Benjamin Stamm. The reduced basis method for the electric field integral equation. *Journal of Computational Physics*, 230(14):5532 – 5555, 2011.
10. Martin W. Hess and Peter Benner. Fast evaluation of time harmonic Maxwell's equations using the reduced basis method. *IEEE Trans. Microwave Theory Techn.*, 61(6):2265–2274, 2013.
11. Laura Iapichino, Alfio Quarteroni, and Gianluigi Rozza. A reduced basis hybrid method for the coupling of parametrized domains represented by fluidic networks. *Computer Methods in Applied Mechanics and Engineering*, 221-222:63–82, May 2012.
12. Yvon Maday and Einar M. Rønquist. A reduced-basis element method. *Journal of Scientific Computing*, 17(1/4):447–459, 2002.
13. Immanuel Maier and Bernard Haasdonk. A Dirichlet-Neumann reduced basis method for homogeneous domain decomposition problems. *Applied Numerical Mathematics*, 78:31–48, 2014.
14. James Clerk Maxwell. On physical lines of force. *The London, Edinburgh, and Dublin Philosophical Magazine and Journal of Science*, 21(139):161–175, 1861.
15. René Milk, Stephan Rave, and Felix Schindler. pyMOR-generic algorithms and interfaces for model order reduction. *accepted for publication in SIAM Journal on Scientific Computing*, 2016.
16. Peter Monk. *Finite element methods for Maxwell's equations*. Oxford University Press, 2003.
17. Jean-Claude Nedelec. Mixed finite elements in r^3 . *Numerische Mathematik*, 35(3):315–341, Sep 1980.
18. Mario Ohlberger and Felix Schindler. Error control for the localized reduced basis multiscale method with adaptive on-line enrichment. *SIAM Journal on Scientific Computing*, 37(6):A2865–A2895, 2015.
19. Dinh Bao Phuong Huynh, David J. Knezevic, and Anthony T. Patera. A static condensation reduced basis element method : approximation and a posteriori error estimation. *ESAIM: Mathematical Modelling and Numerical Analysis*, 47(1):213–251, Nov 2012.
20. Jan Pomplun and Frank Schmidt. Accelerated a posteriori error estimation for the reduced basis method with application to 3d electromagnetic scattering problems. *SIAM Journal on Scientific Computing*, 32(2):498–520, 2010.
21. Theofanis Strouboulis, Ivo Babuška, and Kevin Copps. The design and analysis of the generalized finite element method. *Computer methods in applied mechanics and engineering*, 181(1):43–69, 2000.